

Response to Reviewer's comments for the manuscript bg-2017-151:

"Historic carbon burial spike in an Amazon floodplain lake linked to riparian deforestation near Santarem, Brazil"

Note that the line numbers refer to the revised manuscript.

Editor Comments to the Author:

Your revised version has now been re-evaluated by both original reviewers. As you will see from their comments, both agree that the manuscript has been substantially improved but they also raise a few minor additional comments which should be straightforward to address (Referee # 1) or come back to comments/suggestions that were not adequately addressed (Referee #2, issue of Pu & Pb methodologies to quantify sedimentation rates for both periods considered). I would therefore like to encourage you to revise your manuscript, with particular attention to the issue of sedimentation rates mentioned by Reviewer#2, and provide a detailed response explaining how this is addressed in a new version of the ms.

RESPONSE: We appreciate these construction comments. Below we respond to each comment individually. Note that we have incorporated many of the suggestions on the issue of sedimentation rates as recommended by Reviewer#2. We feel these modifications have strengthened the manuscript substantially.

Reviewer 1

General Comments:

Sanders et al. have revised their manuscript on the organic matter accumulation rates within a floodplain lake in the Amazon. This revised manuscript presents an improved analysis of the data and presentation of methods. In addition to a few small comments below, I have one major question: does any of this impact how these systems should be managed? Currently, neither the abstract nor the conclusion tackle this question. It may not be completely answerable within the scope of this study, but I would welcome an attempt at question of land use management. I believe this would improve the quality of the manuscript, especially as there is significant text spent analyzing the land use change component of this study system.

RESPONSE: We agree and have added the following sentences.

In the abstract:

(Lines 51-53) - "Therefore, this supports the conservation priority of riparian forests as an important management practice for Amazon flooded areas."

In the conclusion:

(Lines 234-235) - “However, any increase of OC burial rates attributed to deforestation might be lower than that loss of terrestrial biomass in the standing crop or soils.”

(Lines 328-329) - “This work supports the urgent need for management practices based on the conservation of riparian forests, demonstrating the spatial dependence of carbon burial capacity of the Amazon floodplain lakes with respect to advances in deforestation in the Basin.”

Specific Comments:

Lines 115-120: I did not catch this in my initial review, but the $\delta^{15}\text{N}$ results should be interpreted with caution based on this pre-treatment method. The relative differences between samples is possibly retained, but the absolute value of $\delta^{15}\text{N}$ following acid pre-treatment is suspect. In addition, C:N can also be affected as acidification and should be interpreted with caution. I do not believe this invalidates the findings here, however these caveats should be considered when interpreting the data.

Here are two recent references that document these issues:

Brodie, C.R., Casford, J.S.L., Lloyd, J.M., Leng, M.J., Heaton, T.H.E., Kendrick, C.P., Yongqiang, Z., 2011. Evidence for bias in C/N, $\delta^{13}\text{C}$ and $\delta^{15}\text{N}$ values of bulk organic matter, and on environmental interpretation, from a lake sedimentary sequence by pre-analysis acid treatment methods. *Quaternary Science Reviews* 30, 3076–3087.

Kim, M.S., Lee, W.S., Suresh Kumar, K., Shin, K.H., Robarge, W., Kim, M., Lee, S.R., 2016. Effects of HCl pretreatment, drying, and storage on the stable isotope ratios of soil and sediment samples. *Rapid Communications in Mass Spectrometry* 1567–1575.

RESPONSE: We agree and have added the following, Line 121-122: “The $\delta^{15}\text{N}$ results and the C/N ratios results should be interpreted with caution based on this pre-treatment method (Brodie et al. 2011).”

Lines 270-283: This fleshed out handling of the statistical methods if welcome. However, I wonder if some of this detail is not better fit for the methods and/or results sections so that the discussion can focus on the implications of the findings.

RESPONSE: We agree and moved these phrases to the Methods section (Line 197 - 204).

Figure 7: Please consider adding a secondary Y-axis indicating the depth associated with the year.

RESPONSE: We agree and the Y-axis to Figure 7 now contains the depth instead of year as also suggested by Reviewer 2.

Reviewer 2

I have reviewed the first version of this paper, and in my first review, I had concerns about the dating methods. Unfortunately, I do not find that the authors have addressed my concerns appropriately in their revision.

RESPONSE: Reviewer 2 raises some valid points in this review of which we feel has improved the manuscript substantially. We detail how we have changed the manuscript in accordance to this Reviewer's suggestions at the end of this comment, as it all relates to the same topic.

The problem is the following: two different dating methods are used, the Pu method and the Pb method.

The Pu method gives information about the average sediment accumulation rate since ~1950, but does not allow for finer temporal resolution. The authors use it in that sense, and that's fine. AD 1950 was located at ~20 cm depth.

The Pb method can resolve temporal changes in sediment accumulation rate at the scale of years, but in the study lake, the authors state that the Pb profile was disturbed in the upper 20 cm, but declining linearly in the 20-60 cm layer. Therefore, they did not calculate sediment accumulation from the Pb data in upper 20 cm of sediment, and they present an average sediment accumulation rate of 4 mm/yr in the 20-60 cm layer.

The chronology given in this paper is therefore (a) an average sediment accumulation rate since 1950 (0-20 cm sediment depth) from the Pu dating, and (b) an average sediment accumulation rate prior to 1950 (20-60 cm sediment depth) from the Pb dating. The presented data does not give information about how sediment accumulation might have varied during the 1950-present period, or during the ~1850-1950 period. Contrary to what the authors claim (L225-227), the fact that the average sediment accumulation rates for these two periods are similar does not indicate that there was little change of sediment accumulation over time; within each of the time periods, sediment accumulation rates might have varied at the scale of years. In fact, when looking at the $^{210}\text{Pb}(\text{ex})$ profile (Fig 4b), there is an intriguing increase in unsupported Pb over the 3-20 cm horizon, possibly indicating non-constant sediment accumulation. Similarly, $^{210}\text{Pb}(\text{ex})$ varies between layers in the 20-60 cm horizon, indicating quite variable sediment accumulation rate, and not a constant sediment accumulation rate, as the authors claim (L212-215).

The lack of time-resolved chronologies is serious when the authors plot chemical data over age (Fig. 7), since there is no information about the exact age each respective layer of sediment. In Figure 7, the authors should instead plot chemical data against sediment depth, and indicate the AD 1950 layer.

The same problem appears when changes in OC burial are attributed to changes in land use (Fig.8B). Over the period where land use change was most intense, e.g. the past 50 years, the authors have only one average value of sediment accumulation rate to rely on, and the values of OC burial cannot be confidently attributed to a certain year. In fact, the calculations of OC burial use one average sediment accumulation rate, and using such averaged OC burial rates to illustrate temporal changes in burial seems unwarranted. Analysis of temporal patterns can only be done with temporally resolved data.

In my opinion, the authors can go two ways: either present the Pb chronologies (i.e. plot depth against age, based on both CIC and CRS models) in order to present evidence for the

attribution of individual sediment layers to certain years. I asked for the Pb chronologies in my first review, but the authors have not responded to that. The other potential way to deal with this issue would be to stay away from giving distinct ages to distinct sediment layers, and analyze the differences between pre-1950 and post-1950 layers (for which there is good data from the Pu dating). The average sediment accumulation rates could still be used to speak about indicative ages, i.e. since the long-term average sediment accumulation was ~4 mm/yr, the 0-4 cm layer may be regarded to represent approximately the past 10 yrs.

Whichever way the authors choose, the ms needs to be revised accordingly prior to publication.

RESPONSE: We have decided to focus the manuscript on general range approximations of the indicative ages, instead of distinct ages to distinct sediment layers as recommended by this Reviewer, i.e., >1930, 1930-1970 and 1970-2010, on Figures 7 and 8A and throughout the manuscript. For instance, Line 39-41: “Historical records from the 1930s and satellite data from the 1970s were used to calculate deforestation rates between 1930 and 1970, and 1970 to 2010 in four zones”. We have also changed Figures 7 and 8 to show depths instead of specific year as suggested. We feel these general age ranges best reflects the uncertainties associated with our sediment dating methods, as noted by this Reviewer.

Furthermore, we now use pre-1950 and post-1950 sedimentation rate estimates for the two separate layers as suggested by the Reviewer, i.e. The $^{239+240}\text{Pu}$ for the rates from near 1950 to present (3.8 mm year^{-1}) and from ~1890 to approximately the 1950s (4.2 mm year^{-1}) as calculated from the $^{210}\text{Pb}_{\text{ex}}$ profiles. These rates for each sediment depth were multiplied by the DBD and OC content for each interval along the entire sediment core.

Another comment: I found the hypothesis a bit vaguely formulated, “related to the carbon burial capacity” leaves room for interpretation. The authors could be more definitive in their prediction: “historically documented increases in deforestation have increased OC burial rates in the studied floodplain lake” or something similar.

RESPONSE: We agree and have changed the hypothesis to the following, Line 95 - 96: “We hypothesize that the historical deforestation in this region of the Amazon may have influenced the OC burial rates in the studied floodplain lake.”

1 **Historic carbon burial spike in an Amazon floodplain lake linked to riparian**
2 **deforestation near Santarem, Brazil**

3
4 Luciana M. Sanders¹, Kathryn Taffs¹, Debra Stokes², Christian J. Sanders³, Alex Enrich-
5 Prast^{4,5}, Leonardo Nogueira Amora^{6,7}, Humberto Marotta^{6,7}

6
7
8
9 ¹*Southern Cross Geoscience, Southern Cross University, P.O. Box 157, Lismore, NSW 2480, Australia.*

10 ²*Marine Ecology Research Centre, Southern Cross University, P.O. Box 157, Lismore, NSW 2480,*
11 *Australia University, P.O. Box 157, Lismore, NSW 2480, Australia.*

12 ³*National Marine Science Centre, School of Environment, Science and Engineering, Southern Cross*
13 *University, Coffs Harbour, New South Wales, Australia.*

14 ⁴*Laboratório de Biogeoquímica, Universidade Federal do Rio de Janeiro (UFRJ), Rio d Janeiro (RJ),*
15 *21941 971, Brazil.*

16 ⁵*Department of Environmental Change, Linköping University, 581 83, Linköping, Sweden.*

17 ⁶*Ecosystems and Global Change Laboratory (LEMG-UFF) / International Laboratory of Global Change*
18 *(LINCGlobal). Biomass and Water Management Research Center (NAB-UFF). Graduated*
19 *Program in Geosciences (Environmental Geochemistry). Universidade Federal Fluminense*
20 *(UFF), Av. Edmundo March, s/nº – Zip Code: 24210-310, Niteroi/RJ- Brazil.*

21 ⁷*Sedimentary and Environmental Processes Laboratory (LAPSA-UFF). Department of Geography.*
22 *Graduated Program in Geography. Universidade Federal Fluminense (UFF), Av. Gal. Milton*
23 *Tavares de Souza, s/nº - Zip Code: 24210-346, Niteroi/RJ- Brazil.*

24
25
26
27
28 *Corresponding author. E-mail address; l.sanders.13@student.scu.edu.au

32 **Abstract**

33 Forests along the Amazon Basin produce significant quantities of organic material, a
34 portion of which is deposited in floodplain lakes. Deforestation in the watershed may
35 then have potentially important effects on the carbon fluxes. In this study, a sediment
36 core was extracted from an Amazon floodplain lake to examine the relationship between
37 carbon burial and land cover/use. Historical records from the 1930s and satellite data
38 from the 1970s were used to calculate deforestation rates between 1930 and 1970, and
39 1970 to 2010 in four zones with different distances from the margins of the lake and its
40 tributaries (100, 500, 1000 and 6000-m buffers). Sediment accumulation rates were
41 determined from the $^{240+239}\text{Pu}$ signatures and the excess ^{210}Pb method, and found to be
42 near 4 mm year⁻¹ for the previous ~120 years. The carbon burial rates ranged between 85
43 and 298 g C m⁻² year⁻¹, with pulses of high carbon burial in the 1950s, originating from
44 the forest vegetation as indicated by $\delta^{13}\text{C}$ and $\delta^{15}\text{N}$ signatures. Our results revealed a
45 potentially important spatial dependence of the OC burial in Amazon lacustrine
46 sediments in relation to deforestation rates in the catchment. These deforestation rates
47 were more intense in the riparian vegetation (100-m buffer) during the period 1930 -
48 1970 and the larger open water areas (500, 1000 and 6000-m buffer) during 1970 - 2010.
49 The continued removal of vegetation from the interior of the forest was not related to the
50 peak of OC burial in the lake, but only the riparian deforestation which peaked during the
51 1950s. Therefore, this supports the conservation priority of riparian forests as an
52 important management practice for Amazon flooded areas. Our novel findings suggest
53 the importance of abrupt and temporary events in which some of the biomass released by
54 the deforestation, especially restricted to areas along open water edges, might reach the
55 depositional environments in the floodplain of the Amazon Basin.

56

57

58 **1. Introduction**

59 Rivers act as vectors, transporting sediment from land to ocean (Abril et al. 2014).
60 Along this trajectory a significant proportion of the sediment load, including organic
61 material, may be deposited in floodplains, creating zones of carbon accumulation (Smith
62 et al. 2002, Dong et al. 2012, Hoffmann et al. 2013). This process is accelerated during
63 flood events, when rivers and tributaries deposit organic material along the inundated
64 floodplains (Smith et al. 2002). In some climate zones, floodplains are seasonally
65 inundated, with riparian zone vegetation dependent upon this seasonal influx of organic
66 material. The riparian vegetation slows water velocity and traps fine-grained, carbon rich
67 sediments within this low-energy environment (Aalto et al. 2003). Therefore, the riparian
68 vegetation along the floodplains may be important for the organic matter deposition and
69 the Amazon carbon cycle.

70 The importance of tropical wetland ecosystems in the carbon cycle is well
71 documented (Downing et al. 1993, Melack et al. 2004, Zocatelli et al. 2013, Abril et al.
72 2014, Marotta et al. 2014). It has been shown that wetlands in the warm tropics are some
73 of the most productive biological communities in the world (Neue et al. 1997),
74 representing an important sink for nutrients (Marotta et al. 2009) and carbon (Peixoto et
75 al. 2016, Sanders et al. 2017), as well as sources of organic substrates to carbon gas
76 production in inland waters (Marotta et al. 2010). However, these wetland ecosystems are
77 also highly threatened by land use activities, especially from deforestation, development
78 of agricultural land and soil degradation (Junk 2013, Lucas et al. 2014).

79 The Amazon Basin wetlands are being degraded by farming activities such as
80 commercial ranching, and an increase in road density (Goulding 1993). Deforestation of

81 the Amazon Basin accelerated toward the end of the 1970's (Skole and Tucker 1993),
82 when an estimated 15% of the pristine rainforest area was lost by the year 2003,
83 increasing to approximately 18% by 2015 (INPE 2016). The ongoing loss of vegetation is
84 responsible for a substantial increase in erosion rates and subsequent sediment inputs into
85 Amazon rivers and lakes (Neill et al. 2013b). Yet these anthropogenic activities are
86 potential sources of allochthonous organic matter that may increase carbon stores in the
87 associated floodplain areas (Diaz and Rosenberg 2008, Stanley et al. 2012).

88 Jupindá Lake provides an ideal opportunity to investigate historical changes in
89 organic carbon burial in a floodplain lake as a result of the well documented
90 anthropogenic activities. This will aid in identifying the still-little known impacts of land
91 cover changes on recent carbon burial rates in depositional environments of the Amazon
92 floodplain. The objectives of this research are to investigate the effects of deforestation
93 and urban development on carbon burial rates in a tropical floodplain lake. We
94 hypothesize that the historical deforestation in this region of the Amazon may have
95 influenced the OC burial rates in the studied floodplain lake.

96

97 **2. Methods**

98 The city of Santarem, in central Amazon, was established in the mid-eighteenth
99 century, approximately 650 km upstream from the Amazon River mouth and at its
100 confluence with the Tapajós River (02°25'0.28"S and 54°42'41.57"W, Figure 1). In 1940,
101 Santarém was only a small village, less than 0.5 km², surrounded by dense pristine
102 rainforest (estimated from the historical mapping of the Santarém City Hall). This city
103 quickly expanded, occupying 5.2 km² by the end of the 1970s and 49.3 km² currently

104 (estimated from satellite images LANDSAT/SRTM). Jupindá Lake is 70 km East of from
105 Santarém City, and receives surface water inflow from small streams draining from the
106 forest and the main tributary Curuá-Una River, a large affluent of the Amazon River
107 (Figure 1). The Lake has been affected by the deforestation associated with the expansion
108 of Santarém City. Between the 1940's and 1950's, there was intense deforestation on the
109 margins of rivers and streams in this area, used to supply the markets with wood and
110 forestry products (Amorim 2000, Cruz et al. 2011). In the 1970s, the Curuá-Una River
111 was dammed (Curuá-Una Dam) 45 km upstream of Jupindá Lake to build the first
112 hydroelectric plant of the Amazon Forest (Ligocki 2003).

113 A 60 cm depth sediment core (diameter 7.5 cm) was collected in 2010 using a gravity
114 corer in the center of the Jupindá Lake (02°27'43.60" S, 54° 5'1.30" W). The sediment
115 core was sub sampled at 2 cm intervals. Dry bulk density (DBD, g cm⁻³) was determined
116 as the dry sediment weight (g) divided by the initial volume (cm³). A homogenized
117 portion was acidified (10% HCl following the procedures outlined in Naidu et al. (2000))
118 to remove carbonate material, then dried and ground to powder for organic carbon (OC),
119 nitrogen (N), $\delta^{13}\text{C}$, and $\delta^{15}\text{N}$ analyses using a Flash Elemental Analyzer coupled to a
120 Thermo Fisher Delta V IRMS (isotope ratio mass spectrometer). The $\delta^{15}\text{N}$ results and the
121 C/N ratios results should be interpreted with caution based on this pre-treatment method
122 (Brodie et al. 2011). Working standards were used (glucose, 10.7 ppt and urea, 41.3 ppt)
123 to calibrate for $\delta^{13}\text{C}$. A pair of standards were measured with every 20 samples. These
124 standards were calibrated initially against international absolute standards LSVEC and
125 NIST8542. Analytical precision: C = 0.1 %, N = 0.1%, $\delta^{13}\text{C}$ = 0.1‰ and $\delta^{15}\text{N}$ = 0.15 ‰.

126 Samples were prepared for Pu dating following the method of Ketterer et al. (2004)
127 with modifications to enable larger sample mass to be processed as a result of the likely
128 lower Pu concentrations in the Southern Hemisphere (Sanders et al. 2016). To obtain a
129 larger mass, sediment intervals were joined and homogenized so the sediment intervals
130 for the $^{240+239}\text{Pu}$ dating was 4 cm intervals. Sample aliquots ranging from 14 to 29 grams
131 were dry-ashed at 600 °C for 16 hours, and leached with 50 mL of 16 M HNO_3 . The
132 leaching was conducted overnight at 80°C with added ^{242}Pu yield tracer (NIST 4334g, 19
133 picograms). Acid leaching (as opposed to complete dissolution with HF) is known to
134 solubilize stratospheric fallout Pu, and there is little possibility that “refractory” HNO_3 -
135 insoluble Pu exists in the South America (Sanders et al. 2014). The leachates were
136 diluted to 100 mL, filtered to remove solids, and the aqueous solutions were processed
137 with TEVA resin (EiChrom, Lisle, IL, USA) in order to chemically isolate 3.0 mL Pu
138 fractions in aqueous ammonium oxalate solution suitable for measurements by sector
139 ICPMS. Pu determinations were performed using a VG Axiom MC operating in the
140 single collector (electron multiplier) mode. The system was used with an APEX HF
141 desolvating micronebulizer system (ESI Scientific, Omaha, NE, USA) with an uptake
142 rate of 0.4 mL/minute. Qualitative mass spectral scans (averages of 50 sweeps over the
143 mass range 237.4 – 242.6) were collected for selected samples prior to the electrostatic
144 sector quantitative scanning of $^{238}\text{U}^+$, $^{239}\text{Pu}^+$, $^{240}\text{Pu}^+$, and $^{242}\text{Pu}^+$. Detection limits were
145 evaluated based upon the analysis of two blanks and considerations regarding the
146 obtained mass spectra. A detection limit of 0.01 Bq/kg of $^{239+240}\text{Pu}$ is applicable for
147 samples of nominal 25 g mass.

148 For ^{210}Pb dating, an intrinsic germanium detector coupled to a multi-channel analyzer
149 was used. Freeze dried and ground sediments were packed and sealed in gamma tubes.
150 Lead-210 and ^{226}Ra activities were calculated by multiplying the counts per minute by a
151 factor that includes the gamma-ray intensity and detector efficiency determined from
152 standard calibrations. Identical geometry was used for all samples. Lead-210 activities
153 were determined by the direct measurement of the 46.5 KeV gamma peak. Radium-226
154 activity was determined via the ^{214}Pb daughter at 351.9 KeV. For ^{226}Ra measurements,
155 the packed samples were set aside for at least 21 days to allow for ^{222}Rn to ingrow and
156 establish secular equilibrium between ^{226}Ra and its granddaughter ^{214}Pb . Excess ^{210}Pb
157 activity was calculated by subtracting the supported ^{210}Pb (i.e., ^{226}Ra activity) from the
158 total ^{210}Pb activity. The sediment accretion rate for the previous 120 years was estimated
159 by two methods derived from ^{210}Pb dating, the Constant Initial Concentration (CIC)
160 model assuming that this rate has not varied during the encompassed time span (Appleby
161 and Oldfield 1992), and the Constant Rate of Supply (CRS) model based on a constant
162 influx of unsupported, atmospheric ^{210}Pb that allows a variable sediment rate (Ivanovich
163 and Harmon 1992). Organic carbon accumulation rates were estimated from an average
164 between these the two dating methods ($^{239+240}\text{Pu}$ and $^{210}\text{Pb}_{\text{ex}}$) the dry bulk density (g cm^{-3})
165 and carbon content for each interval of the entire sediment core.

166 The land/use cover analysis was based on documented historical information before
167 1975 and satellite images (Landsat/SRTM, Table 1) from 1975, 1985, 1995 and 2008
168 available from the United States Geological Survey (USGS). No significant deforestation
169 occurred in the catchment area of the Jupindá Lake until early 1940's (Amorim 2000,
170 Cruz et al. 2011). Subsequent land/use changes were determined using satellite images

171 (Gordon 1980, Munyati 2000). All satellite images were from low-water seasons to
172 remove the influence of the flood pulse on the exposed area over years. The resolution of
173 the images was 30 m, except that from the 1970's which was resampled from 90 to 30 m
174 (Table 1). This approach allowed an assessment of changes in land cover which could
175 then be compared to results from carbon accumulation. Results of the spatial assessment
176 were separated into two time periods; 1930 to 1970, or the timeframe between the onset
177 of land clearing and the first satellite image, and 1970 to 2010 which provides a more
178 detailed assessment of temporal changes to the study area. The time period 1934-1975
179 was characterized by a rapid removal (peak until the 1960's) of vegetation established at
180 the margins of inland waters; especially *Aniba rosaeodora* (Pau-rosa) for extraction of
181 oils, and *Mezilaurus itauba* and *Cedrela fissilis* (Louro-itaúba and Cedro, respectively) as
182 hardwoods, and the opening of clearings for crops of textile fibers and subsistence
183 products. Further, intensification of deforestation towards the interior of the forest and
184 following the urban growth of Santarém is reported from the 1970's (Amorim 2000, Cruz
185 et al. 2011). The depleting vegetal resources near to the margins of lakes and running
186 waters in this region is also well documented (Amorim 2000, Cruz et al. 2011).

187 In order to address the spatial dependence of recent OC burial in Jupindá Lake for
188 deforestation, we analyzed the land/cover use in four buffer areas around this lake and
189 contributing rivers or streams. The first buffer of 100 m represented the riparian forest
190 protected area by the Brazilian laws for fluvial channels with a width of 50 to 200 m.
191 Other buffers were progressively higher, with a width of 500, 1000 and 6000 m from the
192 riverbank and lake margins (Figure 2). In addition, we considered only stretches of rivers
193 and streams 65-km long from Jupindá Lake to analyze its catchment area of more direct

194 influence. This criteria also avoids the interference of the artificial flooding on the
195 margins of the Curuá-Una hydroelectric dam, which was built in 1977 (Fearnside 2005).

196 The statistical treatment of variables and OC burial rates, when grouped into different
197 phases, showed assumptions which required parametric analyses, including normal
198 distribution (Kolmogorov-Smirnov, $p > 0.05$) and homogeneity of variance (Bartlett, $p >$
199 0.05). Thus, we used means and standard errors to represent the distribution of values,
200 and parametric tests were conducted, allowing to compare different phases. Statistical
201 differences were tested using the one-way ANOVA test followed by Tukey's post test
202 (significance was defined as $p < 0.05$). All the statistical tests used in this work were
203 performed using GraphPad Prism 5.0 software.

204

205 3. Results

206 The analyses of $^{239+240}\text{Pu}$ showed no detectable activities from the bottom of the
207 sediment core until the 22-26 cm interval (Figure 3). However, $^{239+240}\text{Pu}$ was detected in
208 the 18-22 cm interval ($0.029 \pm 0.002 \text{ Bq/kg } ^{239+240}\text{Pu}$) with the highest concentrations
209 ($0.047 \pm 0.004 \text{ Bq/kg } ^{239+240}\text{Pu}$) at the 16 cm depth. The $^{239+240}\text{Pu}$ activities appears to
210 spike at the 14 to 18 cm interval, which indicates the 1963 stratospheric fallout peak. It
211 may be said with certainty that the material below 22 cm was deposited pre-bomb (that is,
212 prior to the early 1950's). This affixes an upper limit on the average sedimentation rate of
213 near to 3.8 mm year^{-1} . The Pu atom ratio data indicate that the Pu is originating from
214 stratospheric fallout, i.e. plutonium isotopic ratios ($^{240/239}\text{Pu}$) of ~ 0.18 . These results are
215 consistent with the $^{240}\text{Pu}/^{239}\text{Pu}$ of 0.180 ± 0.014 discussed by Kelley et al. (1999).

216 The ^{210}Pb and ^{226}Ra profiles as well as the $^{210}\text{Pb}_{(\text{ex})}$ profile vs cumulative dry mass

217 accumulation reveals a complex depositional environment with sedimentation variations
218 and disturbances, such as bio-turbation and resuspension in the upper ~ 20 cm of the
219 sediment column (Figure 4). A decrease in $^{210}\text{Pb}_{\text{ex}}$ activity was found below the 20 cm
220 depth interval. The $^{210}\text{Pb}_{\text{ex}}$ data distribution are as follows: $y = -0.0749x + 7.5$; $R^2 = 0.73$;
221 $n=19$; $p < 0.01$ from the 20 to the 60 cm interval, below the apparent mixed zone. Both
222 estimates of sediment accretion rate during the 120 years from CIC and CRS models
223 were similar, reaching 4.1 and 4.3 mm yr^{-1} respectively, which were slightly higher than
224 the ~ 60 year $^{239+240}\text{Pu}$ dates (3.8 mm yr^{-1}). In order to obtain a more reliable estimates of
225 the historical carbon burial rates, the $^{239+240}\text{Pu}$ results, from near 1950 to present, were
226 used (3.8 mm year^{-1}) and $^{210}\text{Pb}_{\text{ex}}$ (4.2 mm year^{-1}) was used from ~1890 to approximately
227 the 1950s. These rates for each sediment depth were multiplied by the DBD and OC
228 content for each interval of the entire sediment core.

229 The dry bulk density (DBD), total organic carbon (OC%), total nitrogen (TN%)
230 content as well as the carbon and nitrogen (C/N) molar ratios along with the $\delta^{13}\text{C}$ and
231 $\delta^{15}\text{N}$ values showed a shift towards the center of the sediment core (Table 2). The
232 relationship between $\delta^{13}\text{C}$ and $\delta^{15}\text{N}$ indicated different origins of OC in the sediment core
233 (Figure 5) contributing to the significant relationship between OC burial and the $\delta^{13}\text{C}$
234 (Figure 6). The significantly greater $\delta^{13}\text{C}$ peak and lower $\delta^{15}\text{N}$ values coupled to higher
235 OC burial rates were observed in the phase between ~1930 to 1970 in Jupindá Lake (one-
236 way ANOVA followed by Tukey's post test, $p < 0.05$; Fig. 7). The $\delta^{13}\text{C}$ values were
237 greater in the phase ~1930 to 1970 in relation to those previous and after respectively
238 (one-way ANOVA followed by Tukey's post test, $p < 0.05$). This peak near 1950 also
239 showed $\delta^{15}\text{N}$ values lower and OC burial rates higher than other phases (one-way

240 ANOVA followed by Tukey's post test, $p < 0.05$).

241 The OC burial rates indicate an increasing trend from ~ 1930 with a peak during the
242 1940's and 50's (grey area in Figure 7). The carbon burial rates increased, from ~186 g
243 $\text{m}^{-2} \text{ year}^{-1}$ before the 1950s, and up to 298 $\text{g m}^{-2} \text{ year}^{-1}$ between the 1940s and 1950s.
244 Carbon accumulation then decreased to approximately 186 $\text{g m}^{-2} \text{ year}^{-1}$ from 1960 to
245 1980, after which a gradual decline in carbon burial is noted. In relation to land use/cover
246 in the surrounding fluvial channels and the Jupindá lake, only the smallest buffer (100 m)
247 showed significant changes during 1930-1970. This time period is when deforestation
248 was nearly 75% higher than in the subsequent time period 1970-2010 (Figure 8a) and
249 when OC burial was greatest ((Figure 8b).

250

251 4. Discussion

252 Similar estimates of sediment accretion were found using different methodologies
253 ($^{239+240}\text{Pu}$ and $^{210}\text{Pb}_{(\text{ex})}$). These accretion rates along with the dry bulk density revealed an
254 insight into changes in the sediment sources of floodplains, and their relationships with
255 changing land cover and land use in the Amazon Basin. The Jupindá Lake showed
256 substantial changes in the carbon burial rates following deforestation, supporting the
257 connection between flooded areas and their surrounding vegetation The high peak in
258 carbon accumulation observed around 1950 appears to be associated with a shift in the
259 source of organic material, inferred by changes in carbon and nitrogen contents and the
260 isotopic fractioning toward the middle (from 20 to 40 cm depth interval) of the sediment
261 column. This peak for different organic and inorganic variables in intermediate depths
262 revealed changes not only in the amount but also in the type of material being deposited

263 over time. Previous studies have reported two common origins for OC in the Amazon
264 forest. Higher $\delta^{15}\text{N}$ and more negative $\delta^{13}\text{C}$ values could indicate the presence of
265 Santarém soil organic matter (such as that adjacent to the Jupindá Lake), while lower
266 $\delta^{15}\text{N}$ and more variable $\delta^{13}\text{C}$ values indicate particulate organic carbon (POC) from the
267 terrestrial vegetation in the catchment (Ometto et al. 2006, Zocatelli et al. 2013). Here, a
268 corresponding increase in OC%, TN% and OC burial rates measured, with a peak near
269 1950, suggesting higher inputs of organic matter into lake. The higher $\delta^{13}\text{C}$ signature,
270 coupled with a lower $\delta^{15}\text{N}$ indicates a greater influence from the terrestrial Amazonian
271 POC during the same period, around 1950 (Ometto et al., 2006).

272 When looking for a cause for this change in the source of organic material, we look to
273 the analysis of land use change. Land clearing associated with early occupation from the
274 1940s in the catchment area of the Jupindá Lake reveals a potential cause of the increased
275 carbon burial observed in this lake. Changes in development use and forestation may
276 significantly affect recent OC burial in mid-high-latitude lakes (Anderson et al. 2013,
277 Dietz et al. 2015). Indeed, our results suggest that land clearing during the 1940's and
278 50's might be related to increased organic matter deposition in the region's floodplain
279 lakes. During this period, intense wood extraction and expansion of agricultural
280 settlements occurred (Amorim 2000, Cruz et al. 2011). One important consequence of
281 deforestation in the watershed is the silting up of lakes (Enea et al. 2012), including
282 those at humid low-latitude areas (Cohen et al. 2005, Bakoariniaina et al. 2006).
283 However, the lake is in a region relatively preserved, and therefore there is no other
284 explanation other than deforestation in the margins to have caused the peak in OC burial
285 near the 1950s. The riparian forest systems are generally effective in reducing the

286 sediment transport by surface runoff, with the removal of this vegetation increasing the
287 erosion processes especially in the Amazon Basin as a result of intense rainfall (Neill et
288 al. 2013a). The peak of the significantly greater $\delta^{13}\text{C}$ and lower $\delta^{15}\text{N}$ values coupled to
289 higher OC burial rates were observed in the phase between ~1930 to 1970 in Jupindá
290 Lake (one-way ANOVA followed by Tukey's post test, $p < 0.05$; Fig. 7). The $\delta^{13}\text{C}$ values
291 were greater in the ~1930 to 1970 phase as related to those previous and after
292 respectively (one-way ANOVA followed by Tukey's post test, $p < 0.05$). This peak
293 between ~1930 to 1970 also showed delta $\delta^{15}\text{N}$ values lower and OC burial rates higher
294 than other phases (one-way ANOVA followed by Tukey's post test, $p < 0.05$).

295 We also found a spatial dependence of the carbon accumulation in the Lake Jupindá,
296 as the much lower OC burial was coupled to higher deforestation rates in those larger
297 buffers around its margins and main fluvial channels (500, 1000 and 6000 m) in the
298 period after 1970s (between the ~1970s to 2010) than that before (~1930 to 1970). This
299 confirms previous evidences that the recent deforestation process in the region was
300 started in areas near running and lake waters (Amorim 2000, Cruz et al. 2011), and not in
301 the interior of the forest. The enhanced OC burial in lacustrine sediments before ~1970
302 was related to higher deforestation rates only in the riparian vegetation zone (100-m
303 buffers), suggesting a higher influence of deforestation with decreasing distance to water
304 courses. Therefore, the soil carbon enrichment to the aquatic sediments during the peaks
305 of riparian deforestation may cause intense but temporary carbon burial events in the
306 Amazon floodplain, representing potentially only a significant part of the total loss of
307 terrestrial organic matter. In addition, the continued removal of vegetation from the

308 | interior of the forest might not be directly related to increases of OC burial, even
309 | temporarily, in depositional aquatic ecosystems.

310

311 | **5. Conclusion**

312 | Palaeolimnological techniques were used with a historical spatial analysis of
313 | deforestation to interpret changes in sediment characteristics during the past century.

314 | The Pu dating method closely approximates measurements from the ^{210}Pb chronologies
315 | and hence offers mechanism to determine sedimentation rates and carbon accumulation
316 | in Amazon sediments. An increase in OC burial, up to 298 OC g m⁻² year⁻¹, coincides
317 | with changes in the $\delta^{13}\text{C}$ and $\delta^{15}\text{N}$ signatures, likely influenced by the heavy deforestation
318 | in riparian systems of this region during the 1940s and 1950s. It is suggested that the net
319 | increase in carbon burial towards the center of the sediment core, which represents the
320 | highest carbon burial rates during the 1950s, is a result of a change in source of organic
321 | matter deposition. However, any increase of OC burial rates attributed to deforestation
322 | might be lower than the loss of terrestrial biomass in the standing crop or soils. The
323 | differing carbon burial rates along the sediment core therefore reveals the potential
324 | complexity of the Amazon floodplain lakes, directly related to the development within
325 | the Basin. The differing carbon burial rates along the sediment core therefore identify the
326 | potential complexity of the Amazon floodplain lakes, directly related to the development
327 | within the Basin. This work supports the urgent need for management practices based on
328 | the conservation of riparian forests, demonstrating the spatial dependence of carbon
329 | burial capacity of the Amazon floodplain lakes with respect to advances in deforestation
330 | in the Basin.

331

332

333

334 **Acknowledgements**

335 LMS is supported by an APA and IPRS scholarships. HM received a research grant from
336 the Brazilian Research Council (CNPq – “Programa Universal”) and the Research
337 Support Foundation of the State of Rio de Janeiro (FAPERJ – “Programa Jovem Cientista
338 do Nosso Estado”). CJS is supported by the Australian Research Council
339 (DE160100443).

340

341 **CAPTIONS TO FIGURES**

342 **Figure 1.** Floodplain Lake where the sediment core was collect, near the Amazon River
343 and the city of Santarém, Brazil. This floodplain lake has a diameter of approximately 3
344 km.

345 **Figure 2.** Different buffer sizes (100m, 500m, 1km and 6km) along the stretch of the
346 Curuá-Una river from Jupindá Lake (red) to the hydroelectric dam upstream (yellow).

347 **Figure 3.** $^{239+240}\text{Pu}$ profile, indicating ~ 1950 when these radionuclides were first
348 introduced into the atmosphere.

349 **Figure 4.** Lead-210 (black circles) and ^{226}Ra (white circles) profiles against depth. Grey
350 squares represent the $^{210}\text{Pb}(\text{ex})$ profile vs cumulative dry mass.

351 **Figure 5.** $\delta^{13}\text{C}$ vs $\delta^{15}\text{N}$. The Amazon River POM and Santarem soil organic matter
352 values, adjacent to the study area, are taken from Zocatelli et al (2013).

353 **Figure 6.** Carbon burial as a function of $\delta^{13}\text{C}$ and $\delta^{15}\text{N}$.

354 | **Figure 7.** $\delta^{13}\text{C}$, $\delta^{15}\text{N}$ and carbon burial rate values in relation to age-depth (year:cm).
 355 | Panels below each vertical profile represent respective data grouped by the three general
 356 | phases >19341930, 19341930-19705 and 19705-201008. Filled square symbols
 357 | represent means of a given variable in each sediment layer, and the vertical bars show the
 358 | mean with the standard deviation of the respective phase. Equal letters in each panel
 359 | represent non-significant differences ($p > 0.05$, one-way ANOVA followed by Tukey's
 360 | post test).

361 | **Figure 8.** Percentage of modified areas in relation to the different buffers (Panel A).
 362 | Carbon burial (black dots) and changes in the riparian vegetation (two grey bars represent
 363 | the two general phases) as related to time (Panel B).

364

365 | **CAPTION TO TABLES**

366 | **Table 1.** Satellite acquisition data from United States Geological Survey (USGS) and the
 367 | Curuá-Una River quota from Brazilian Water Agency (ANA).

368 | **Table 2.** Depth profiles of dry bulk density (DBD), total organic carbon (OC%), total
 369 | nitrogen (TN%) carbon and nitrogen (C/N) molar ratios, $\delta^{13}\text{C}$ and $\delta^{15}\text{N}$.

370
 371
 372
 373
 374
 375

Table 1.

<i>Month/Year</i>	<i>Landsat Data</i>	<i>Curuá-Una River Quota</i>
Aug/1975	2	5.3
Oct/1985	5	3.7
June/1995	5	6
June/2008	5	No data

376
 377

378 **Table 2.**
379

Depth (cm)	DBD (g cm ⁻³)	$\delta^{15}\text{N}$	$\delta^{13}\text{C}$	C (%)	N (%)	C/N
0-2	1.0	8.9	-29.2	3.8	0.3	17.2
2-4	0.9	11.7	-29.0	3.8	0.3	18.7
4-6	1.0	10.4	-28.8	4.0	0.3	19.2
6-8	1.1	9.3	-28.7	4.3	0.3	20.2
8-10	1.0	9.4	-28.7	4.1	0.3	19.8
10-12	1.1	7.9	-28.6	4.6	0.3	21.2
12-14	1.1	8.2	-28.7	4.3	0.3	19.9
14-16	1.1	7.8	-28.6	4.3	0.3	20.9
16-18	1.0	8.7	-28.5	4.4	0.3	21.2
18-20	1.1	7.5	-28.4	4.4	0.3	19.8
20-22	1.0	6.5	-28.2	5.4	0.3	21.2
22-24	1.0	6.0	-27.8	5.3	0.3	21.5
24-26	1.0	5.2	-27.4	7.3	0.4	25.4
26-28	1.1	6.1	-27.6	6.0	0.3	23.8
28-30	1.0	5.0	-27.3	6.0	0.4	22.7
30-32	1.0	5.4	-28.0	6.1	0.3	27.0
32-34	1.3	6.6	-28.5	4.4	0.2	27.5
34-36	1.6	8.9	-29.0	2.2	0.1	23.1
36-38	1.4	11.4	-29.4	2.9	0.1	30.4
38-40	1.4	10.4	-29.5	3.3	0.1	30.5
40-42	1.5	11.4	-29.3	2.4	0.1	23.8
42-44	1.6	12.2	-29.4	1.3	0.1	15.6
44-46	1.8	8.2	-29.6	1.2	0.1	14.3
46-48	1.5	8.8	-29.8	2.2	0.1	21.6
48-50	0.9	10.4	-29.7	2.9	0.2	25.6
50-52	0.9	10.2	-29.7	2.6	0.1	27.2
52-54	0.9	7.1	-29.7	3.9	0.2	28.6
54-56	0.9	9.2	-29.9	3.6	0.2	27.8
56-58	0.9	6.6	-30.1	4.3	0.2	30.1
58-60	0.9	5.0	-30.1	3.5	0.2	23.1
Average	1.11	8.34	-28.9	4.0	0.2	23.0
Stand Dev	0.24	2.1	0.8	1.9	0.1	4.2

380
381
382
383
384
385
386
387
388
389
390
391
392
393
394

395 **References**

- 396
397 Aalto, R., L. Maurice-Bourgoin, T. Dunne, D. R. Montgomery, C. A. Nittrouer, and J. L.
398 Guyot. 2003. Episodic sediment accumulation on Amazonian flood plains
399 influenced by El Niño/Southern Oscillation. *Nature* **425**:493-497.
- 400 Abril, G., J. M. Martinez, L. F. Artigas, P. Moreira-Turcq, M. F. Benedetti, L. Vidal, T.
401 Meziane, J. H. Kim, M. C. Bernardes, N. Savoye, J. Deborde, E. L. Souza, P.
402 Albéric, M. F. Landim De Souza, and F. Roland. 2014. Amazon River carbon
403 dioxide outgassing fuelled by wetlands. *Nature* **505**:395-398.
- 404 Amorim, A. T. d. S. 2000. Santarém: uma síntese histórica, Canoas, Ulbra, Santarem,
405 Brazil
- 406 Anderson, N. J., R. D. Dietz, and D. R. Engstrom. 2013. Land-use change, not climate,
407 controls organic carbon burial in lakes. *Proceedings. Biological sciences / The*
408 *Royal Society* **280**:20131278.
- 409 Appleby, P. G., and F. Oldfield. 1992. Application of lead-210 to sedimentation studies.
410 Pages 731-783 in M. Ivanovich and S. Harmon, editors. *Uranium Series*
411 *Disequilibrium: Application to Earth, Marine and Environmental Science*. Oxford
412 Science Publications.
- 413 Bakoariniaina, L. N., T. Kusky, and T. Raharimahefa. 2006. Disappearing Lake Alaotra:
414 Monitoring catastrophic erosion, waterway silting, and land degradation hazards
415 in Madagascar using Landsat imagery. *Journal of African Earth Sciences* **44**:241-
416 252.
- 417 Brodie, C. R., J. S. L. Casford, J. M. Lloyd, M. J. Leng, T. Heaton, C. P. Kendrick, and
418 Z. Yongqiang. 2011. Evidence for bias in C/N, $\delta^{13}\text{C}$ and $\delta^{15}\text{N}$ values of bulk
419 organic matter, and on environmental interpretation, from a lake sedimentary

420 sequence by pre-analysis acid treatment methods. *Quaternary Science Reviews*
421 **30**:3076-3087.

422 Cohen, A. S., M. R. Palacios-Fest, J. McGill, P. W. Swarzenski, D. Verschuren, R.
423 Sinyinza, T. Songori, B. Kakagozo, M. Syampila, C. M. O'Reilly, and S. R. Alin.
424 2005. Paleolimnological investigations of anthropogenic environmental change in
425 Lake Tanganyika: I. An introduction to the project. *Journal of Paleolimnology*
426 **34**:1-18.

427 Cruz, H., P. Sablayrolles, M. Kanashiro, and M. S. Amaral, P. 2011. Relação empresa/
428 comunidade no manejo florestal comunitário e familiar: Uma contribuição do
429 Projeto Floresta em pé.

430 Diaz, R. J., and R. Rosenberg. 2008. Spreading dead zones and consequences for marine
431 ecosystems. *Science* **321**:926-929.

432 Dietz, R. D., D. R. Engstrom, and N. J. Anderson. 2015. Patterns and drivers of change in
433 organic carbon burial across a diverse landscape: Insights from 116 Minnesota
434 lakes. *Global Biogeochemical Cycles* **29**:708-727.

435 Dong, X., N. J. Anderson, X. Yang, X. chen, and J. Shen. 2012. Carbon burial by shallow
436 lakes on the Yangtze floodplain and its relevance to regional carbon sequestration.
437 *Global Change Biology* **18**:2205-2217.

438 Downing, J. P., M. Meybeck, J. C. Orr, R. R. Twilley, and H. W. Scharpenseel. 1993.
439 Land and water interface zones. *Water, Air, & Soil Pollution* **70**:123-137.

440 Enea, A., G. Romanescu, and C. Stoleriu. 2012 Quantitative considerations concerning
441 the source-areas for the silting of the red lake (Romania) lacustrine basin.
442 . Romania.

443 Fearnside, P. M. 2005. Do hydroelectric dams mitigate global warming? The case of
444 Brazil's Curuá-Una Dam. *Mitigation and Adaptation Strategies for Global Change*
445 **10**:675-691.

446 Gordon, S. I. 1980. Utilizing LANDSAT imagery to monitor land-use change: A case
447 study in ohio. *Remote Sensing of Environment* **9**:189-196.

448 Goulding, M. 1993. Flooded forests of the Amazon. *Scientific American* **268**:114-
449 120+115.

450 Hoffmann, T., M. Schlummer, B. Notebaert, G. Verstraeten, and O. Korup. 2013. Carbon
451 burial in soil sediments from Holocene agricultural erosion, Central Europe.
452 *Global Biogeochemical Cycles* **27**:828-835.

453 INPE. 2016. Program for the Estimation of Amazon Deforestation. Accessed 20
454 November 2016, http://www.obt.inpe.br/prodes/prodes_1988_2015n.htm.

455 Ivanovich, M., and S. Harmon. 1992. Uranium Series Disequilibrium - Applications to
456 Earth, Marine and Environmental Sciences. second edition edition. Oxford
457 Science Publications.

458 Junk, W. J. 2013. Current state of knowledge regarding South America wetlands and
459 their future under global climate change. *Aquatic Sciences* **75**:113-131.

460 Ketterer, M. E., K. M. Hafer, V. J. Jones, and P. G. Appleby. 2004. Rapid dating of
461 recent sediments in Loch Ness: Inductively coupled plasma mass spectrometric
462 measurements of global fallout plutonium. *Science of the Total Environment*
463 **322**:221-229.

464 LigockI, L. P. 2003. Comportamento geotécnico da barragem de Curuá-Una, Pará. Rio de
465 Janeiro.

466 Lucas, C. M., J. Schöngart, P. Sheikh, F. Wittmann, M. T. F. Piedade, and D. G.
467 McGrath. 2014. Effects of land-use and hydroperiod on aboveground biomass and
468 productivity of secondary Amazonian floodplain forests. *Forest Ecology and*
469 *Management* **319**:116-127.

470 Marotta, H., L. Bento, F. A. De Esteves, and A. Enrich-Prast. 2009. Whole ecosystem
471 evidence of eutrophication enhancement by wetland dredging in a shallow
472 Tropical Lake. *Estuaries and Coasts* **32**:654-660.

473 Marotta, H., C. M. Duarte, F. Meirelles-Pereira, L. Bento, F. A. Esteves, and A. Enrich-
474 Prast. 2010. Long-term CO₂ variability in two shallow tropical lakes experiencing
475 episodic eutrophication and acidification events. *Ecosystems* **13**:382-392.

476 Marotta, H., L. Pinho, C. Gudas, D. Bastviken, L. J. Tranvik, and A. Enrich-Prast. 2014.
477 Greenhouse gas production in low-latitude lake sediments responds strongly to
478 warming. *Nature Climate Change* **4**:467-470.

479 Melack, J. M., L. L. Hess, M. Gastil, B. R. Forsberg, S. K. Hamilton, I. B. T. Lima, and
480 E. M. L. M. Novo. 2004. Regionalization of methane emissions in the Amazon
481 Basin with microwave remote sensing. *Global Change Biology* **10**:530-544.

482 Munyati, C. 2000. Wetland change detection on the Kafue Flats, Zambia, by
483 classification of a multitemporal remote sensing image dataset. *International*
484 *Journal of Remote Sensing* **21**:1787-1806.

485 Naidu, A. S., L. W. Cooper, B. P. Finney, R. W. Macdonald, C. Alexander, and I. P.
486 Semiletov. 2000. Organic carbon isotope ratio ($\delta^{13}\text{C}$) of Arctic Amerasian
487 Continental shelf sediments. *International Journal of Earth Sciences* **89**:522-532.

488 Neill, C., M. T. Coe, S. H. Riskin, A. V. Krusche, H. Elsenbeer, M. N. Macedo, R.
489 McHorney, P. Lefebvre, E. A. Davidson, R. Scheffler, A. M. e Silva Figueira, S.
490 Porder, and L. A. Deegan. 2013a. Watershed responses to Amazon soya bean
491 cropland expansion and intensification. *Philosophical Transactions of the Royal*
492 *Society B: Biological Sciences* **368**.

493 Neill, C., M. T. Coe, S. H. Riskin, A. V. Krusche, H. Elsenbeer, M. N. Macedo, R.
494 McHorney, P. Lefebvre, E. A. Davidson, R. Scheffler, A. M. Figueira, S. Porder,
495 and L. A. Deegan. 2013b. Watershed responses to Amazon soya bean cropland
496 expansion and intensification. *Philosophical transactions of the Royal Society of*
497 *London. Series B, Biological sciences* **368**:20120425.

498 Neue, H. U., J. L. Gaunt, Z. P. Wang, P. Becker-Heidmann, and C. Quijano. 1997.
499 Carbon in tropical wetlands. *Geoderma* **79**:163-185.

500 Ometto, J. P. H. B., J. R. Ehleringer, T. F. Domingues, J. A. Berry, F. Y. Ishida, E.
501 Mazzi, N. Higuchi, L. B. Flanagan, G. B. Nardoto, and L. A. Martinelli. 2006.
502 The stable carbon and nitrogen isotopic composition of vegetation in tropical
503 forests of the Amazon Basin, Brazil. *Biogeochemistry* **79**:251-274.

504 Peixoto, R. B., H. Marotta, D. Bastviken, and A. Enrich-Prast. 2016. Floating Aquatic
505 Macrophytes Can Substantially Offset Open Water CO₂ Emissions
506 from Tropical Floodplain Lake Ecosystems. *Ecosystems* **19**:724-736.

507 Sanders, C. J., B. D. Eyre, I. R. Santos, W. MacHado, W. Luiz-Silva, J. M. Smoak, J. L.
508 Breithaupt, M. E. Ketterer, L. Sanders, H. Marotta, and E. Silva-Filho. 2014.
509 Elevated rates of organic carbon, nitrogen, and phosphorus accumulation in a
510 highly impacted mangrove wetland. *Geophysical Research Letters* **41**:2475-2480.

511 Sanders, C. J., I. R. Santos, D. T. Maher, J. L. Breithaupt, J. M. Smoak, M. Ketterer, M.
512 Call, L. Sanders, and B. D. Eyre. 2016. Examining $^{239+240}\text{Pu}$, ^{210}Pb and
513 historical events to determine carbon, nitrogen and phosphorus burial in
514 mangrove sediments of Moreton Bay, Australia. *Journal of Environmental*
515 *Radioactivity* **151**:623-629.

516 Sanders, L. M., K. H. Taffs, D. J. Stokes, C. J. Sanders, J. M. Smoak, A. Enrich-Prast, P.
517 Macklin, I. R. Santos, and H. Marotta. 2017. Carbon accumulation in Amazonian
518 floodplain lakes: A significant component of Amazon budgets? *Limnology &*
519 *Oceanography Letters*:29-35.

520 Skole, D., and C. Tucker. 1993. Tropical deforestation and habitat fragmentation in the
521 amazon: Satellite data from 1978 to 1988. *Science* **260**:1905-1910.

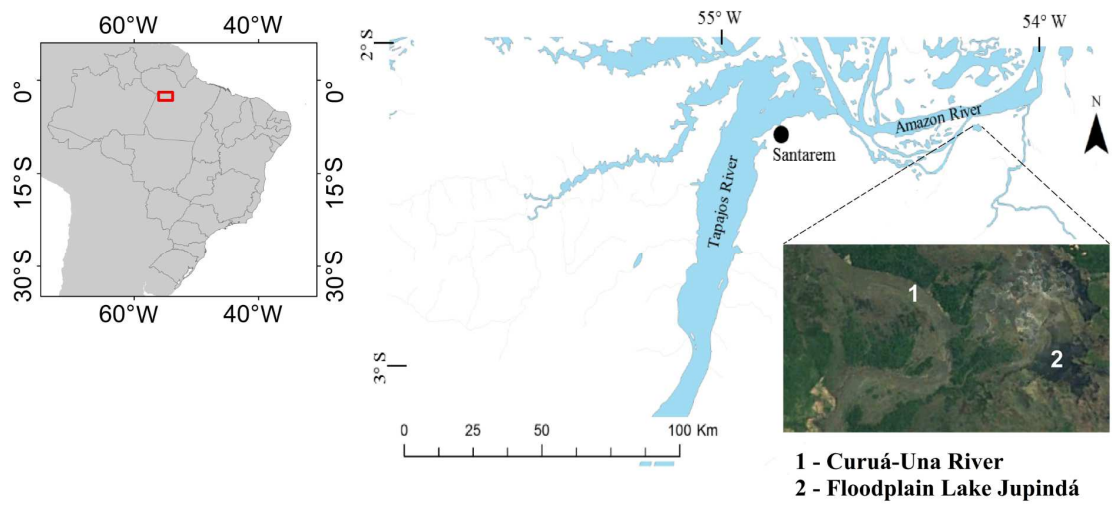
522 Smith, L. K., J. M. Melack, and D. E. Hammond. 2002. Carbon, nitrogen, and
523 phosphorus content and ^{210}Pb -derived burial rates in sediments of an Amazon
524 floodplain lake. *Amazoniana* **17**:413-436.

525 Stanley, E. H., S. M. Powers, N. R. Lottig, I. Buffam, and J. T. Crawford. 2012.
526 Contemporary changes in dissolved organic carbon (DOC) in human-dominated
527 rivers: Is there a role for DOC management? *Freshwater Biology* **57**:26-42.

528 Zocatelli, R., P. Moreira-Turcq, M. Bernardes, B. Turcq, R. C. Cordeiro, S. Gogo, J. R.
529 Disnar, and M. Boussafir. 2013. Sedimentary evidence of soil organic matter
530 input to the curuai amazonian floodplain. *Organic Geochemistry* **63**:40-47.

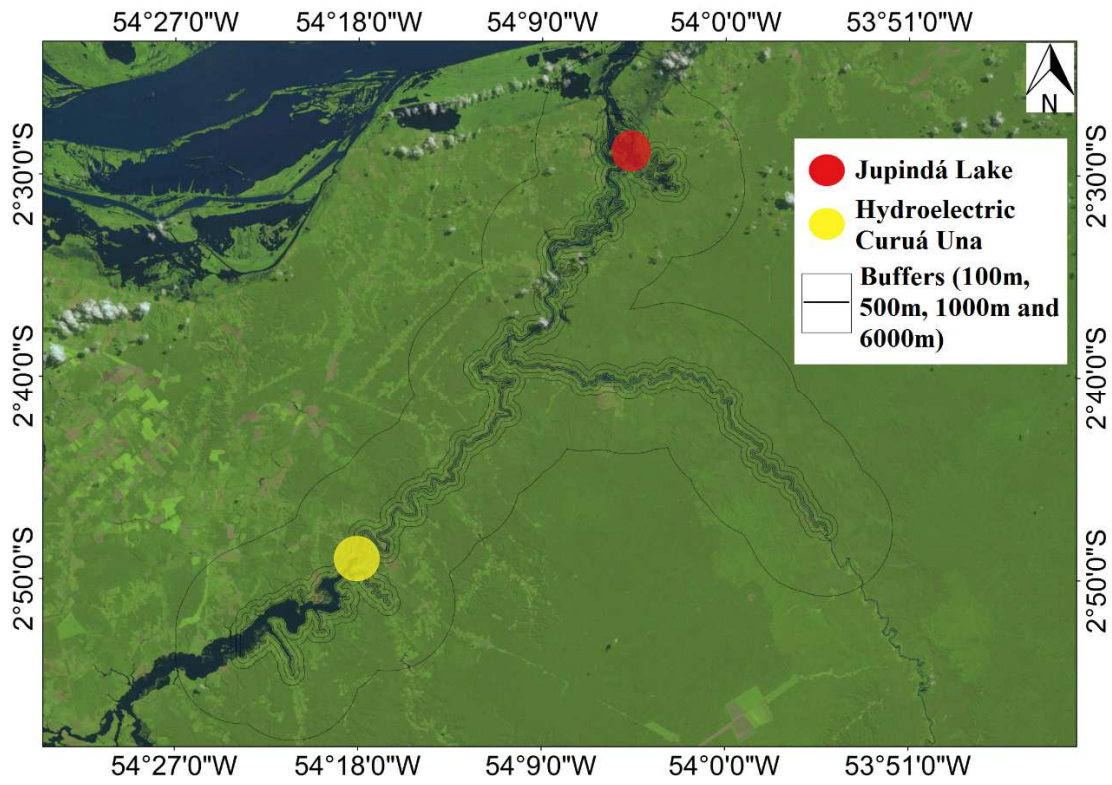
531
532
533
534

535 **Figure 1.**



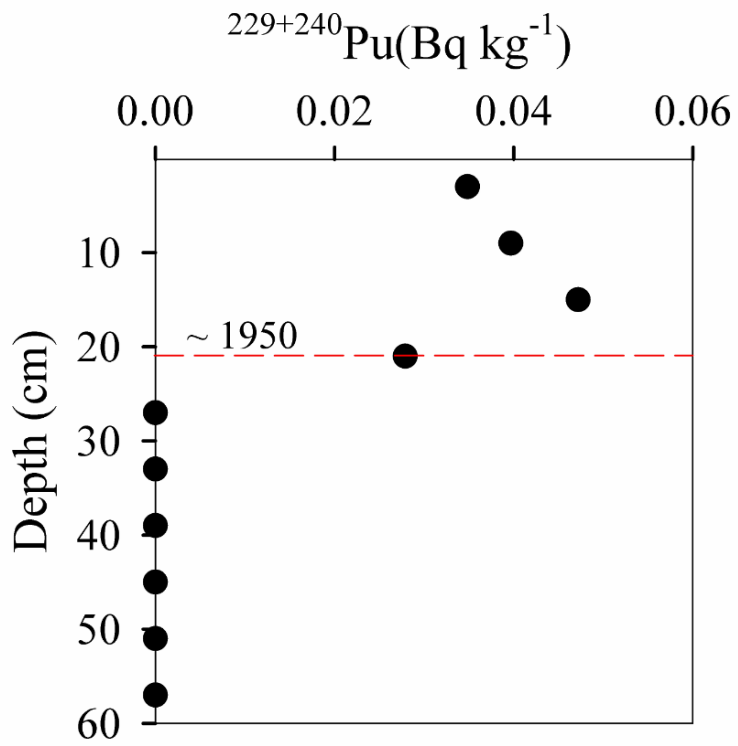
536
537
538
539
540
541
542
543
544
545
546
547
548
549
550
551
552
553
554
555
556
557
558
559
560
561
562
563
564
565
566

567 **Figure 2.**



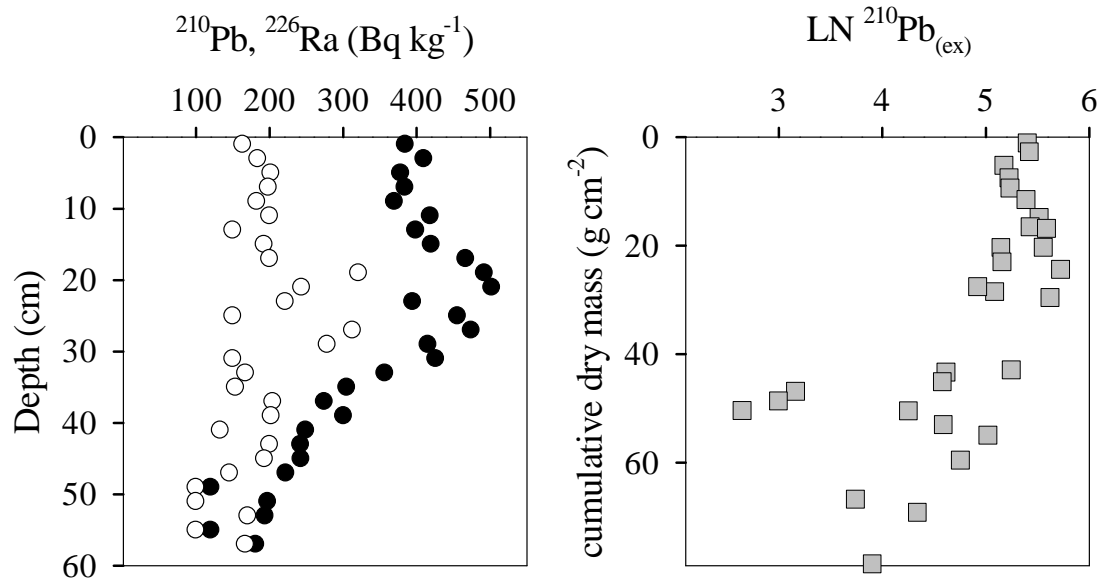
568
569
570
571
572
573
574
575
576
577
578
579
580
581
582
583
584
585
586
587
588
589
590
591

592 **Figure 3.**



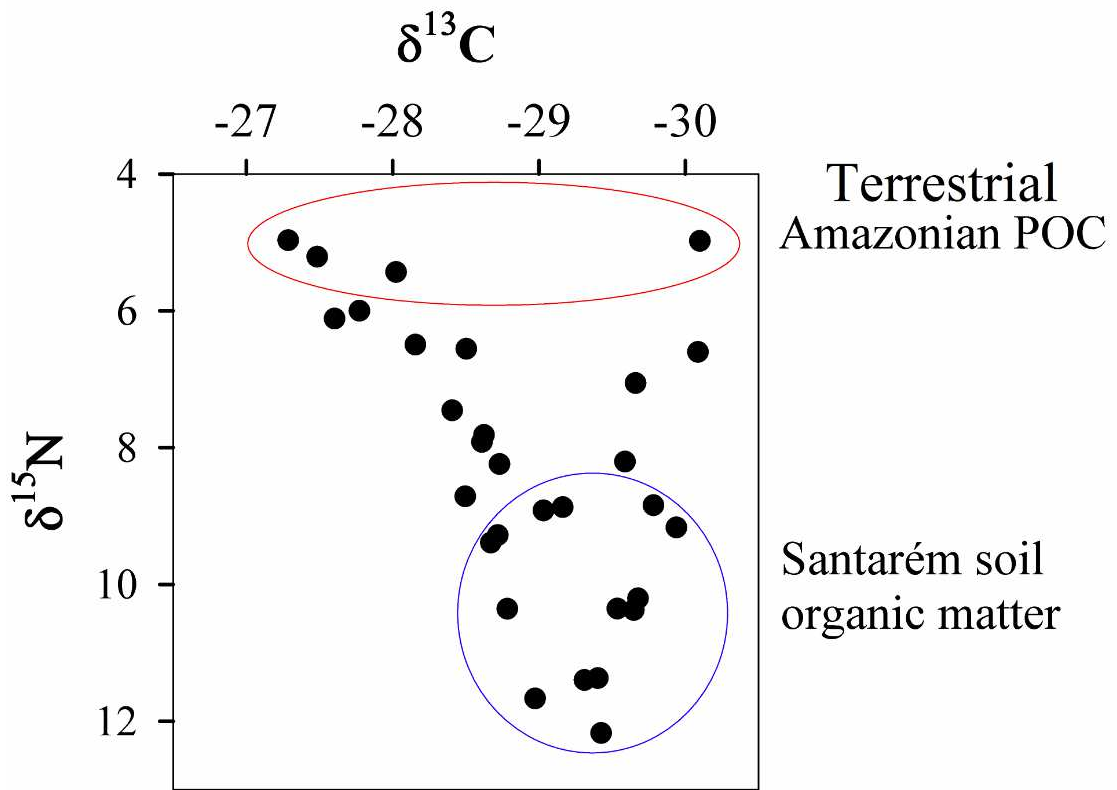
593
594
595
596
597
598
599
600
601
602
603
604
605
606
607
608
609
610
611
612
613
614
615
616

617 **Figure 4.**
618



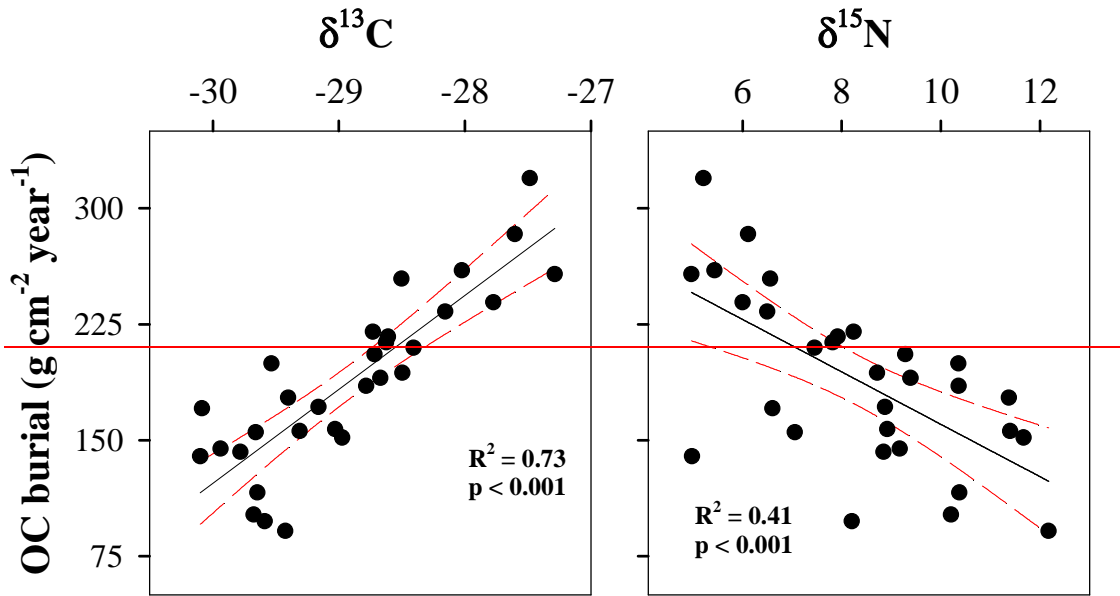
619
620
621
622
623
624
625
626
627
628
629
630
631
632
633
634
635
636
637
638
639
640
641
642
643
644
645
646
647

648 **Figure 5.**



649
650
651
652
653
654
655
656
657
658
659
660
661
662
663
664
665
666
667
668
669
670
671

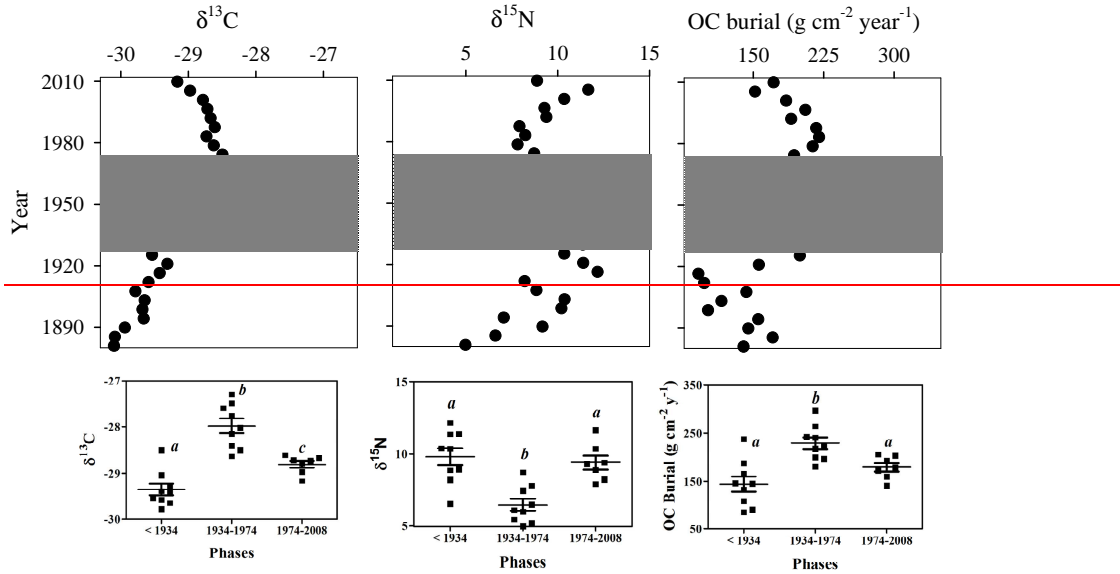
672 **Figure 6.**



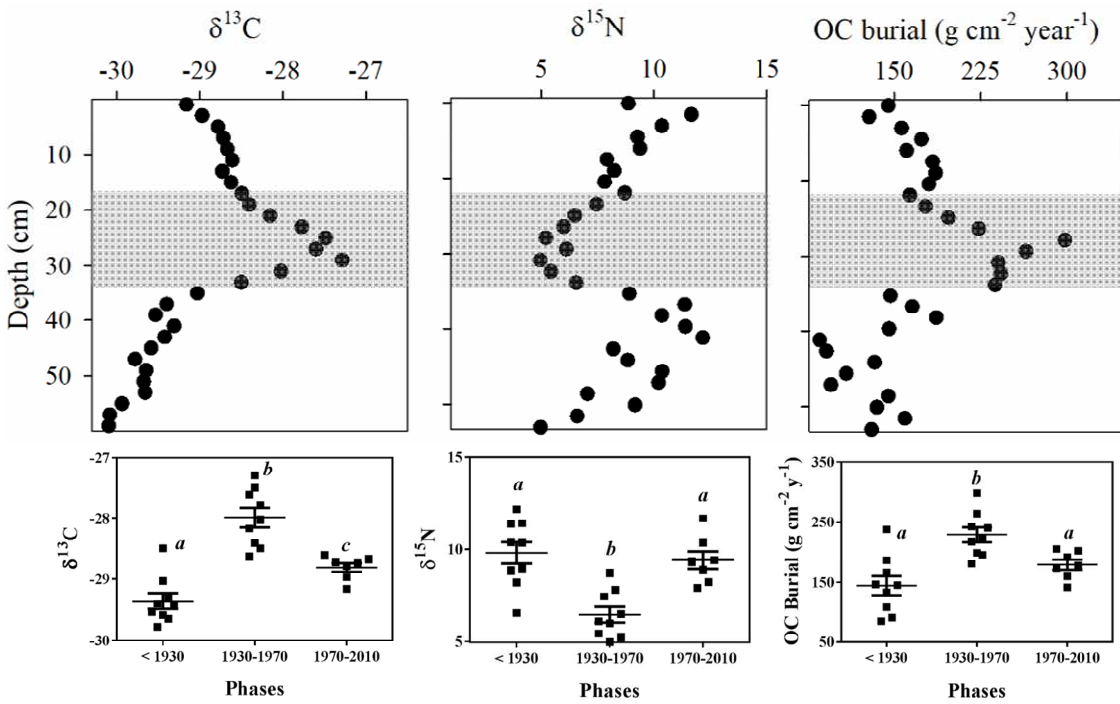
673
674
675
676
677
678
679
680
681
682
683
684
685
686
687
688
689
690
691
692
693
694
695
696
697
698
699

700

Figure 7.



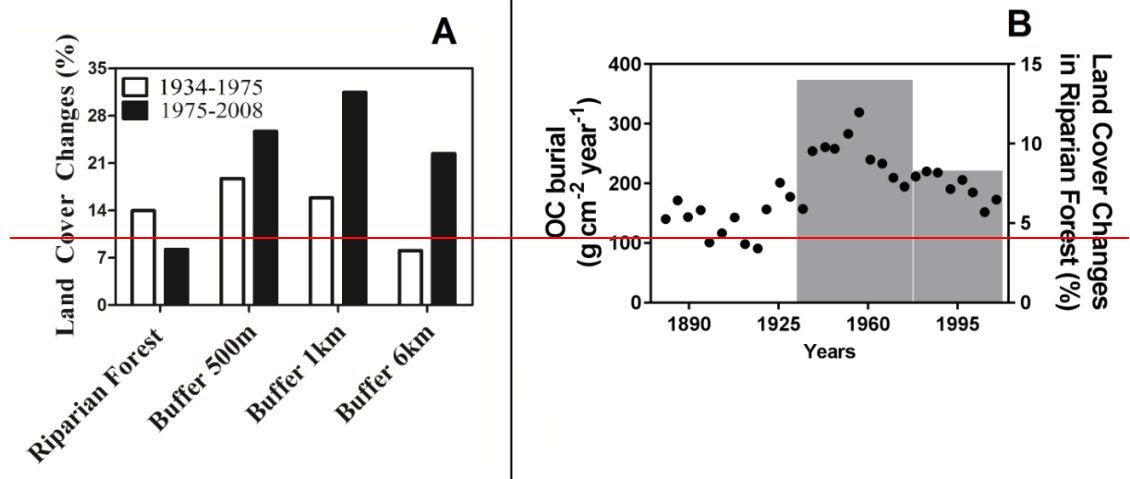
701
702
703
704



705
706
707
708
709
710
711
712

713
714
715
716
717
718
719
720
721
722
723
724
725
726
727
728
729
730
731
732

Figure 8.



733
734

